Journal of Statistical Physics, Vol. 63, Nos. 1/2, 1991

High-Density Properties of Hard Spheres within a Modified Percus–Yevick Theory: The Role of Thermodynamic Consistency

P. V. Giaquinta,[1] G. Giunta,[1] and G. Malescio[1]

Received August 3, 1990; final December 5, 1990

Using an integral-equation approach based upon an approximation for the tail function, the equilibrium properties of a system of hard spheres are studied with special concern for the behavior in the region of close packing. The closure adopted is such that full, internal consistency is ensured in the thermodynamics of the model with respect to both the two zero-separation theorems as well as to the more standard virial and fluctuation routes to the equation of state. The scheme also makes use of the continuity properties of the tail function and of the cavity distribution function at contact. These properties are explictly tested in the low-density limit up to the fourth derivative. The theory generates an equilibrium branch bounded on the high-density side by a point corresponding to a packing fraction $\eta \simeq 0.78$, a value which closely matches Rogers' least upper bound for the densest packing of spheres. The pair structure of the fluid in the state of random close packing is also compared to the type of local order predicted by the theory at similar densities.

KEY WORDS: Hard spheres; tail function; zero-separation theorems; self-consistent theory; equation of state; random close packing; closest packing.

1. INTRODUCTION

In this paper we revisit a self-consistent Ornstein–Zernike (OZ) approach to the structure and thermodynamics of hard spheres[1,2] and analyze in deeper detail the predictions offered by the theory in the high packing regime.

In the absence of the exact solution of the model but for one dimension, an old but still debated question which bears far-reaching implica-

[1] Istituto di Fisica Teorica, Universita' degli Studi di Messina, C. P. 50, 98166 Villaggio S. Agata (Messina), Italy.

0022-4715/91/0400-0141$06.50/0

tions is whether an equilibrium statistical mechanical theory for a classical continuous system of hard spheres should exhibit a natural breakdown (in the form, say, of some divergence undergone by the thermodynamic properties) at the highest density allowed by Euclidean geometry for an ordered crystal configuration or, instead, at the lower *random* close-packing (RCP) density, which then would mark the end of the (metastable) overcompressed fluid branch.[2] Of course, the deeper underlying question is how the claimed discontinuous fluid-to-solid transition which has been almost undoubtedly assessed by numerical simulation experiments[6] for a finite system with periodic boundary conditions would eventually show up in the *exact* canonical partition function after a properly taken thermodynamic limit. Furthermore, it is not even clear whether and where any signature whatsoever of the RCP threshold would thereby emerge as well. Unfortunately, at such high densities numerical experiments progressively meet with growing difficulties in sampling—over the time scale of the simulation—the equilibrium state of the system pertaining to a given set of thermodynamic parameters. Therefore, the resulting information may not necessarily be consistent with the results obtained by use of integral equation theories which, on their own, start to be plagued, in such a regime, by quite serious shortcomings which make any prediction almost completely unreliable. In this contest, the most venerable approximation used for dealing with structural correlations in a model system of hard spheres, viz., the one proposed by Percus and Yevick[7] (PY) and solved analytically by Wertheim[8] and Thiele,[9] leads to a divergence in the equation of state (EOS) at a relative packing fraction $\eta_{\max}^{\mathrm{PY}} = 1$, while the highest physically accepted value for this quantity in three dimensions is $\eta_{\mathrm{CP}} = \pi\sqrt{2}/6$, corresponding to a face-centered cubic (FCC) or hexagonal closest-packing (HCP) crystal arrangement of spheres. On the other hand, at $\eta_{\min}^{\mathrm{PY}} \simeq 0.61$, indeed just below the currently estimated RCP fraction $\eta_{\mathrm{RCP}} = 0.64 \pm 0.02$,[10] the PY radial distribution function (RDF) $g(r)$ starts to attain negative values in the region of the first minimum, an occurrence which obviously conflicts with the very definition of the RDF itself. One question which seems natural at this point is how the two features depend upon the chosen integral closure and, more specifically, upon the intrinsic ambiguity rooted in the thermodynamics of the model. In fact, the *virial* and *fluctuation* routes to the pressure are known to yield different results in the PY approximation, and such a discrepancy grows rapidly with the density.[11] It is then reasonable to wonder whether an augmented PY theory, conveniently modified in its basic ansatz so as to ensure complete thermodynamic consistency at the level of structural pair correlations,

[2] Recent contributions explicitly addressing this point are given in refs. 3–5.

would lead to more sensible predictions on approaching the close-packing regime. In particular, the evolution with more refined closures of the gap marked by the densities corresponding to $\eta_{\max}^{PY}$ and $\eta_{\min}^{PY}$ in the PY approximation might also yield hints of some relevance for the questions outlined above. It is in this direction that the present work tries to give a contribution, aiming, in the very least, at accomplishing a finer understanding of the role played by thermodynamic consistency in an integral equation approach to the study of the liquid state.

2. AN APPROXIMATION FOR THE TAIL FUNCTION

The Percus–Yevick approximation for a single-component fluid of hard spheres consists in assuming that the direct correlation function (DCR) entering the OZ equation

$$h(r) = c(r) + \rho \int d\mathbf{r}'\, h(|\mathbf{r} - \mathbf{r}'|)\, c(r') \tag{1}$$

vanishes outside the core diameter σ:

$$c_{PY}(r) = 0, \qquad r > \sigma \tag{2}$$

In Eq. (1), ρ is the particle number density and $h(r) = g(r) - 1$ is the total correlation function, which, as a consequence of the impenetrability of the particle core, on its own satisfies the exact condition

$$h(r) = -1, \qquad r < \sigma \tag{3}$$

The assumption made in Eq. (2) is notoriously a rather crude understatement over the space decay of the hard-sphere $c(r)$ as calculated via numerical simulation experiments.[12] The most prominent feature that Eq. (2) is missing is the positive tail of the DCF outside the core. In fact, on increasing the packing of the spheres, a peak develops at $r = \sigma^+$ which becomes sharper and sharper with the density. For states of the system below the freezing point, this tail substantially decays to zero for distances $r \gtrsim 2\sigma$. The rationale behind the presence of such a feature in the DCF can be qualitatively explained upon thinking of $-k_B T c(r)$ (where k_B is Boltzmann's constant and T is the temperature) as an effective potential in a scheme *à la* Percus.[3] In this picture, it can be easily understood that the

[3] This potential can be actually associated with the virtual presence in the fluid of an extra pseudocomponent of highly diluted "field-generating" particles producing locally a density profile equivalent to the relative spatial arrangement autonomously exploited by the reference system and properly characterized via its bulk RDF (see, for instance, ref. 13).

short-ranged tail outside the core does in fact mimic a net average attraction acting between a couple of spheres in spite of the absence of any attractive interaction in the Hamiltonian. This effect is the result of a collective interplay involving all of the remaining particles which induce a topological confinement of the tagged pair with a strength that is clearly enhanced by an increase of the density of the system.

The simplest way to model this feature in the DCF dates back to Waisman,[14] who proposed a Yukawa form for the DCF outside the core:

$$c_W(r) = \frac{K}{r/\sigma} \exp[-z(r-\sigma)], \qquad r > \sigma \tag{4}$$

This approximation is in fact appealing, as it leads to an analytical solution of the OZ equation for the DCF inside the core in a "variational space" spanned by two free parameters, K and the inverse range parameter z, respectively. Waisman determined these two quantities by forcing the thermodynamics of the model as calculated via the virial and compressibility routes to reproduce the experimental results parametrized by the Carnahan and Starling (CS) EOS.[15] This procedure is, however, conceptually unsatisfactory, since one needs an *external* input to evaluate the parameters as a function of $\eta \equiv (\pi/6)\,\rho\sigma^3$. As a result, the theory does not possess full predictive power, merely achieving a realistic parametrization of the structural properties of the fluid. On the other hand, in order to set up a totally self-contained scheme, one would need two equations to fix K and z, and the requirement of *internal* consistency between the virial and fluctuation routes to the EOS does not clearly suffice by itself for this. A way to overcome this difficulty, as originally proposed in ref. 1, is to resort to the two zero-separation theorems[16,17] which lead to a small-r expansion for the cavity distribution function $y(r)$ in the form

$$\ln y(r) = \beta\mu^{ex} - \frac{3}{2}\left(\frac{\beta P^{ex}}{\rho}\right)\frac{r}{\sigma} + \cdots \tag{5}$$

where $y(r) = \exp[\beta u(r)]\, g(r)$, $u(r)$ is the interatomic potential, $\beta = 1/k_B T$, and μ^{ex} and P^{ex} are the excess parts of the chemical potential and pressure, respectively. Equation (5) provides in principle other two consistency constraints for the thermodynamics of the system, but requires the knowledge of $y(r)$ inside the core. This information can be mapped equivalently onto that for the "tail function" $d(r) \equiv c(r) + y(r) - g(r)$, which for hard spheres takes the form

$$d(r) = \begin{cases} y(r) + c(r), & r \leqslant \sigma \\ c(r), & r \geqslant \sigma \end{cases} \tag{6}$$

The tail function, at variance with the behavior of both $g(r)$ and $c(r)$, is known to be continuous at $r=\sigma$. This property rests upon the demonstrated continuity at contact of the cavity distribution function[9] and of the function $\Theta(r) \equiv y(r) - d(r)$.[18] This latter result is quite general and follows from the OZ equation which also implies the Fourier transform of $d(r)$ to be positive semidefinite.[19]

In ref. 1 the authors, modifying a suggestion originally due to Henderson and Grundke,[20] proposed the following functional parametrization for the tail function:

$$d(x) = \begin{cases} K \exp\left(\sum_{n=1}^{N} \alpha_n (x-1)^n \right), & x \leqslant 1 \\ c_{\mathrm{W}}(x), & x \geqslant 1 \end{cases} \tag{7}$$

where $x = r/\sigma$. In that paper, the upper summation index N was set equal to 3. For this reason, from now on we shall refer to that version of the theory as SCT(3) [i.e., self-consistent theory (3)].

Equation (7) is still kept as the starting point for the present analysis of the structure and thermodynamics of a model system of hard spheres.

3. THERMODYNAMIC CONSISTENCY IN THE HØYE AND STELL SCHEME

Given Eqs. (3) and (7), the OZ equation can be explicitly reduced, in the scheme exploited by Høye and Stell,[21] to a pair of equations for the Yukawa parameters z and K in the form

$$z = z[\eta, a, y(1)] \tag{8}$$

$$K = K[\eta, z, a, y(1)] \tag{9}$$

where $y(1)$ is the contact value of the cavity distribution function and

$$a \equiv 1 - 24\eta \int_0^\infty c(x)\, x^2\, dx \tag{10}$$

Hence, in this scheme, the structural properties a and $y(1)$ replace z and K in the role of basic primitive quantities. While referring the reader to the original paper by Høye and Stell for a complete analysis of the solution of the OZ equation, we just report here Eq. (8) in its explicit form, as it will turn out to be useful in the following:

$$z = -\frac{2}{(1-\eta)^3\, \Delta a} \left(6\eta(1-\eta)^2\, \Delta y(1) \sqrt{a} + (1+2\eta) \right.$$
$$\left. \times \{6\eta\, \Delta y(1)[6\eta\, \Delta y(1) - (1-\eta)^2\, \Delta a]\}^{1/2} \right) \tag{11}$$

where

$$\Delta y(1) = y(1) - y_{\mathrm{v}}^{\mathrm{PY}}(1) \tag{12}$$

$$\Delta a = a - a_{\mathrm{f}}^{\mathrm{PY}} \tag{13}$$

and $y_{\mathrm{v}}^{\mathrm{PY}}(1) = (1+\eta/2)(1-\eta)^{-2}$ and $a_{\mathrm{f}}^{\mathrm{PY}} = (1+2\eta)^2(1-\eta)^{-4}$ are the PY virial and fluctuation expressions for $y(1)$ and a, respectively.

All of the quantities entering the Waisman solution for the DCF inside the core can then be expressed in closed analytical form as functions of η, z, K, a, and $y(1)$. However, our approximation for the tail function calls into play $N+2$ unknown parameters which need to be uniquely specified. As anticipated in the preceding section, the basic criterion introduced in ref. 1 was to require complete thermodynamic consistency at the level of pair correlation functions.

In the first place, the equivalence between the virial and fluctuation routes to the equation of state leads to a differential constraint in the form

$$a(\eta) = 1 + \frac{\partial}{\partial \eta}\left[4\eta^2 y(1)\right] \tag{14}$$

On the other hand, from the short-distance behavior of $y(x)$ it follows that the following conditions should also be satisfied:

$$\begin{aligned} d(0) &= K \exp\left(\sum_{n=1}^{N} (-1)^n \alpha_n(\eta)\right) \\ &= \exp(\beta\mu^{\mathrm{ex}}) + c(0) \end{aligned} \tag{15}$$

and

$$\begin{aligned} d'(0) &= \left(\sum_{n=1}^{N} (-1)^{n-1} n\alpha_n(\eta)\right) d(0) \\ &= 6\eta y(1) \exp(\beta\mu^{\mathrm{ex}}) - c'(0) \end{aligned} \tag{16}$$

where $d'(0) \equiv [\partial d(x)/\partial x]_{x=0}$.

Upon integrating the virial equation of state, one finds for the excess chemical potential

$$\beta\mu^{\mathrm{ex}} = \left(4\eta y(1) + 4\int_0^{\eta} y(1)\, d\eta\right) \tag{17}$$

From the OZ equation applied to a system of particles with a hard core we get for the DCF and its space derivative at the origin

$$c(0) = -[a(\eta) + v(\eta)] \tag{18}$$

$$c'(0) = 6\eta[y(1)]^2 \tag{19}$$

where

$$v(\eta) \equiv 24\eta \int_1^\infty c(x)\, g(x)\, x^2\, dx \tag{20}$$

Equation (19) has been recently proven in an extended form by Zhou and Stell.[22] However, being a general consequence of the specific integral structure of the OZ equation, it is also tautologically satisfied by every OZ-based theory and, in particular, by the Waisman approximation, as can be easily verified via an explicit calculation of $c'_w(x)$ at $x=0$. As far as the quantity $v(\eta)$ is concerned, in the present scheme it becomes the Laplace transform of the RDF and its expression in terms of η, z, K, a, and $y(1)$ can be found in ref. 21.

Upon using Eqs. (17) and (18), one can put Eqs. (15) and (16) in the form

$$\sum_{n=1}^{N} (-1)^n \alpha_n(\eta) = -\ln K + \beta\mu^{ex} + \ln\{1 - [a(\eta) + v(\eta)] \exp(-\beta\mu^{ex})\} \tag{21}$$

$$\sum_{n=1}^{N} (-1)^{n-1} n\alpha_n(\eta) = -\{6\eta y(1)[1 - y(1) \exp(-\beta\mu^{ex})]\} \times \{1 - [a(\eta) + v(\eta)] \exp(-\beta\mu^{ex})\}^{-1} \tag{22}$$

where the right-hand side of both equations is now a (highly nonlinear) functional of those quantities only upon which the Høye and Stell solution of the OZ equation is constructed. Equations (14), (21), and (22) constitute our basic thermodynamic closure of the model. However, this set of equations will possibly admit a unique solution only if in Eq. (7) the upper summation index N is set equal to one. Unfortunately, it is not difficult to verify, at least in the low-density regime, that such a choice on the overall shape of the tail function inside the core is not flexible enough to support simultaneously the above thermodynamic constraints and does ultimately lead to unphysical results. At lowest order in η the tail function and its derivative at $x=0$ are[2,20,22]

$$d(0) = 17\eta^2 + \cdots \tag{23}$$

$$d'(0) = -33\eta^2 + \cdots \tag{24}$$

From Eqs. (15) and (16) we thus get for α_1 and K within SCT(1)

$$\alpha_1^{(0)} \equiv \alpha_1(\eta \to 0) = -33/17 \tag{25}$$

and

$$K(\eta) = K_2 \eta^2 + \cdots \tag{26a}$$

with

$$K_2 = [17 \exp(-33/17)] \tag{26b}$$

On the other hand, in order for the inverse range parameter z to be real and positive in the limit of $\eta \to 0$, the second-order coefficient K_2 is restricted to lie in the range (see the Appendix)

$$0 \leqslant K_2 \leqslant \tfrac{3}{4} \tag{27}$$

The boundary values in Eq. (27) do in fact correspond to the two distinct estimates which would be obtained for K_2 via the OZ equation upon using the PY approximation for calculating the contact value of the RDF through the virial and fluctuation routes, respectively. The twofold condition on K_2 is visibly violated from the upper-bound side by the value obtained for this quantity within SCT(1). We thus need to extend the upper summation index in Eq. (7) up to $N = 2$, at the very least. However, for every new parameter besides K, z, and α_1 we need one extra equation as well. To this end, as moreover suggested in ref. 1, we shall further exploit the continuity properties of the tail function and, in particular, of its spatial derivatives at contact.

4. ON THE CONTINUITY OF THE TAIL FUNCTION AT CONTACT

As is well known, upon taking into explicit account the finite discontinuity induced by the hard-core potential on both the RDF and DCF at $x = 1$, it is possible to show via the OZ equation that the function $\Theta(x) = y(x) - d(x)$, and correspondingly $y(x)$ and $d(x)$ as well, are piecewise analytic with discontinuities in the derivatives at $x = 2, 3, 4, \ldots$.[8,9] In particular, it also follows that $\Theta(x)$ is continuous at contact with its first two derivatives, while as far as the third derivative is concerned, we find

$$\Delta\Theta'''(1) \equiv \Theta'''(1^+) - \Theta'''(1^-) = -24\eta y(1)\, \Delta c'(2) \tag{28}$$

Note, however, that at $x = 2$ the function $\Theta(x)$ turns out to be continuous with its first derivative. Hence, in the absence of more specific information on the exact behavior of the DCF outside the core, it may be plausible to assume that $y(x)$ and $d(x)$, too, are *separately* continuous with their first derivatives. Should this be the case, the continuity of $\Theta(x)$ at $x = 1$ would

extend up to the third derivative, as, moreover, is usually stated in the literature.[4] But again, as a matter of principle, these results on the continuity at contact of $\Theta(x)$ together with its first three derivatives cannot be expected to hold necessarily also for $y(x)$ and $d(x)$ taken separately.[5] However, at least in the limit of low densities, the continuity of the tail function at $x=1$ can be proven *exactly* up to its third derivative. In fact, as already noted, the density expansion of the tail function does actually start from order ρ^2 and may be expressed as[23]

$$d(x)=\sum_{n\geqslant 2} d_n(x) \tag{29}$$

In particular, the second-order contribution turns out to be given by the sum of the following connected simple graphs:

$d_2(x) =$ 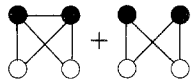 (30)

where each line represents a Mayer f-bond, with $f(x)\equiv\exp[-\beta u(x)]-1$. These graphs have also been calculated exactly. Actually, they lead to two *different* analytical expressions whose domain of validity is confined to inside[24] or outside the core,[25] respectively. As expected, the two branches join at $x=1$. The resulting $d_2(x)$ turns out to be a positive, continuous, and monotonously decaying function, which, moreover, vanishes identically for distances larger than $\sqrt{3}$.

We have indeed verified the continuity of the first three derivatives of $d_2(x)$ at contact. Their expressions are particularly messy and respectably lengthy, so that we shall not report them here. The continuity of the tail function actually break downs with its fourth derivative, which has a discontinuity whose value is found to be

$$\Delta d_2''''(1)=144\eta^2 \tag{31}$$

Correspondingly, it is possible to verify that the fourth derivative of $y(x)$ has an equivalent discontinuity at $x=1$ (but for an opposite sign). The resulting discontinuity in the difference function $\Theta(x)$ does indeed reproduce the result which can be calculated independently after expanding

[4] This statement is manifestly true in any *approximation* which rests on a fully analytical form for the DCF outside the core, as, for instance, in the PY theory (see, in this respect, ref. 9). However, Percus[18] claims that for hard spheres the continuity of $\Theta(x)$ at contact with its first three derivatives is a general consequence of the OZ equation.

[5] In ref. 20, Henderson and Grundke, on building up their phenomenological ansatz for the cavity distribution function, actually invoke the continuity of the first derivative of $y(x)$ at contact. However, the authors are not aware of any general proof of this statement either for the first derivative or for the second and third derivatives.

to order η^2 the exact expression of $\Delta\Theta''''(1)$. In fact, for this quantity we find

$$\Delta\Theta''''(1) \equiv -288\eta^2[y(1)]^3 + 24\eta[\Delta c'(2)\cdot y'(1) - \Delta c''(2)\cdot y(1)] \quad (32)$$

Note that, as, moreover, has been already remarked, the DCF (and thus any potential discontinuity exhibited by this function at $x=2$) vanishes identically for $x \geqslant \sqrt{3}$ up to second order in η. Therefore, any contribution to $\Delta\Theta''''(1)$ which might arise from the second term on the rhs of Eq. (32) would eventually show up only at order η^4.

5. HIERARCHICAL SOLUTION OF THE THEORY: FOURTH VIRIAL COEFFICIENT

In order to bypass the physical inconsistencies manifested by the present theory at the level configured with SCT(1), we shall model the form of the tail function inside the core in a more flexible way by extending the range of the summation in the argument of the exponential so as to include a number of terms $N \geqslant 2$ [see Eq. (7)]. The extra free parameters from the set $\{\alpha_n\}$ which thus come into play are determined by extrapolating the continuity at contact of the first $(N-1)$ derivatives of the tail function (with $N \leqslant 4$) outside the low-density domain throughout the whole accessible region of the phase diagram. It is readily seen that the above condition imposed on $d'(x)$ leads to

$$\alpha_1 = -(1+z) \quad (33)$$

while α_2 is left "free," together with the Yukawa parameters K and z, to saturate the constraints provided by Eqs. (14), (21), and (22). This scheme will be referred to as SCT(2). Upon pushing ahead this procedure, we obtain

$$\alpha_2 = 1/2 \quad (34)$$

which, together with Eq. (33) and α_3 used to match the thermodynamic closure, defines SCT(3).[6] Finally, the last continuity condition imposed upon the third derivative leads to the scheme SCT(4) with α_4 "free" and

$$\alpha_3 = -1/3 \quad (35)$$

while α_1 and α_2 are given by Eqs. (33) and (34), respectively.

[6] In ref. 22, Zhou and Stell finally analyze the results obtained within an approximate theory whose structure is utterly equivalent to that of SCT(3) apart from the condition on the continuity of the second derivative of the tail function at contact. The missing equation is replaced by an external assumption for the EOS of the system, which is parametrized as an *ad hoc* mixture of the virial and fluctuation equations of state provided by the PY approximation. Hence, their procedure is not self-contained and, consequently, is not homogeneous with our approach at any level of the approximation.

The first comment which immediately arises after looking at Eqs. (33)–(35) is that only α_1 actually shows a density dependence via the inverse range parameter z. Therefore, it is reasonable to expect that the higher order schemes, i.e., SCT(3) and SCT(4), should behave somehow worse than SCT(2) because of their inability to follow the density evolution of the model with the parameters α_2 and α_3, respectively. Indeed, it appears that within SCT(2) and SCT(3) the Yukawa ansatz for the DCF outside the core is too simple as compared to the shape of increasing complexity for $d(x)$ inside the core, at least as far as the local properties beyond the first derivative are concerned. Therefore, upon pushing the theory beyond the SCT(2) level, no new independent information on the structure of the model should be gained. These considerations may be explicitly substantiated by comparing, for example, the values of the fourth virial coefficient B_4 which are obtained in the three schemes. In fact, the theory does correctly reproduce the first three coefficients of the virial series independently of the chosen closure. We refer the reader to the Appendix for more details on the calculations; we note that the exact value of B_4 is[11]

$$B_4/(\tfrac{1}{4}B_2)^3 = 18.3648... \tag{36}$$

where $B_2 = \frac{2}{3}\pi\sigma^3$ is the second virial coefficient. We also note that the two PY values for the above quantity are 16 and 19, respectively, depending on whether the virial or fluctuation route is followed for the calculation, while the value implied by the Carnahan and Starling EOS[15] is 18. In Table I we report the estimates obtained within SCT, which also fall short of the exact value. However, the deviation is definitely less than 2% within SCT(2), even lower than that corresponding to the CS assumption. The error made by SCT increases slightly with the level of the approximation, consistent with the previous considerations on the relative predictive

Table I. Fourth Virial Coefficient and $\eta \to 0$ Limit of the Inverse Range Parameter z

Theory	$B_4/(\frac{1}{4}B_2)^3$	$z^{(0)}$
Exact	18.364...	6.450[a]
SCT(1)	—	—
SCT(2)	18.054	4.058
SCT(3)	17.853	3.184
SCT(4)	17.737	2.799

[a] This value is obtained from Eq. (A.1) using the exact value of B_4.

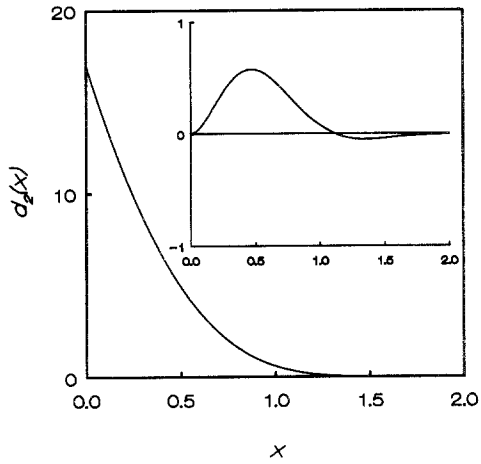

Fig. 1. The function $d_2(x)$. The inset shows the difference between this quantity and its corresponding approximate form within SCT(2).

capacity offered by the three schemes. Figure 1 shows the difference between the exact $d_2(x)$ and its approximation within SCT(2). The theory, while underestimating this function inside the core, shows a slower spatial decay for $x \gtrsim 1.12$ with a vanishing tail extending beyond $\sqrt{3}$.

6. BREAKDOWN OF THE THEORY AT HIGH DENSITIES

The OZ equation with a DCF of Yukawa form outside the core retains the PY singularity at $\eta = 1$. Actually, it is easy to show that a generic "physical" solution of the one-Yukawa OZ theory (i.e., before any constraint whatsoever is imposed in order to fix both K and z) cannot exhibit any divergence for a value of the packing fraction strictly less than one. In fact, it is clear from Eq. (11) that the condition $z > 0$, ensuring the correct asymptotic behavior of the DCF for $x \geqslant 1$, may be unconditionally satisfied in the range $0 \leqslant \eta \leqslant 1$ only if

$$y(1) > y_{\mathrm{v}}^{\mathrm{PY}}(1) \tag{37}$$

and

$$a < a_{\mathrm{f}}^{\mathrm{PY}} \tag{38}$$

Precisely this last condition on the inverse compressibility removes the possibility of a divergence of both $y(1)$ and a for $\eta < 1$. Such a shortcoming is the result of the ansatz made for the DCF outside the core. Therefore,

a one-Yukawa theory does not yet contain all the necessary elements which would make it possible to model in a correct way the behavior of the system at the point of maximum packing where the pressure has to diverge. However, it can also be shown that the generalized closure exploited in this paper does indeed force the theory to break down before the terminal singularity at $\eta = 1$ can be ultimately approached. In fact, the physical branch is bound to be eventually discontinued as the result of the impossibility for the solution to satisfy *simultaneously* for $\eta \to 1^-$ all of the constraints discussed above about the consistency between thermodynamics and structure and the continuity of the tail function at contact. At high densities, Eqs. (21) and (22) for the consistency inside the core asymptotically reduce to

$$\alpha_1 - \alpha_2 \simeq \ln K - \beta\mu^{ex} \tag{39}$$

$$\alpha_1 - 2\alpha_2 \simeq -6\eta y(1) \tag{40}$$

From Eq. (33), ensuring the continuity of $d'(x)$ at $x = 1$, we then find for z

$$z \simeq -1 - 2\ln K + 2y(1) + 8\int_0^\eta y(1)\, d\eta \tag{41}$$

where use has been made of Eq. (17) for the excess chemical potential. On the other hand, the continuity of the function $\Theta(x)$ supplemented with Eq. (6) yields for K

$$K = y(1) + c(1^-) \tag{42}$$

Since the quantity $c(1^-)$ is negative, it follows from Eq. (40) that in the limit of $\eta \to 1^-$ the strength of the Yukawa tail K is bound to diverge as $y(1)$ at the most. Therefore, on the basis of some general constraints pertaining to the consistency between structure and thermodynamics and to the continuity properties of correlation functions at $x = 1$, the spatial decay rate of the DCF outside the core should asymptotically behave as

$$z \simeq 2y(1) \tag{43}$$

since both $\ln K$ and the integral on the rhs of Eq. (39) will eventually diverge, for η sufficiently close to 1, less rapidly than $y(1)$.

However, it is not difficult to verify that, given the boundary conditions (37) and (38) for the solution of the OZ integral equation, the asymptotic behavior of z which may be predicted in the limit of $\eta \to 1^-$ through Eq. (11) is

$$z \simeq 4(1-\eta)\, y(1) \tag{44}$$

Quite clearly, Eqs. (43) and (44) cannot hold together. Hence, the present theory will lead to an acceptable physical solution under the constraints discussed above only over a restricted domain $0 \leqslant \eta \leqslant \eta_{\max}^{\mathrm{SCT}}$ with $\eta_{\max}^{\mathrm{SCT}} < 1$.

7. NUMERICAL ALGORITHM

Independently of the order of the approximation set for $d(\mathrm{x})$ inside the core, one has to solve the coupled set of Eqs. (14), (21), and (22) with K, z, and α_N playing the role of unknown primitive quantities, the residual coefficients $\alpha_{(n<N)}$ [whose number depends on the chosen scheme SCT(N)] being determined through Eqs. (33)–(35). The scheme is solved by an iterative procedure, starting from some initial guess for the thermodynamics of the system (e.g., the CS phenomenological EOS). Given at the ith cycle (with $i = 1, 2, \ldots$) the iterant $[y(1)]_i$ evaluated in a range $\{0, \eta\}$ over a grid of equispaced points, we first compute the quantities a_i and $(\beta\mu^{\mathrm{ex}})_i$ through Eqs. (14) and (17), respectively, using standard routines for the differentiation and integration of a tabulated function. The next iterant $[y(1)]_{i+1}$ is then obtained from Eqs. (21) and (22), which are solved numerically for $y(1)$ and α_N. New values for the inverse compressibility and excess chemical potential a_{i+1} and $(\beta\mu^{\mathrm{ex}})_{i+1}$ are calculated from $[y(1)]_{i+1}$ and used as input for the next cycle. This procedure is iterated until the demanded convergence rate of the thermodynamic output is achieved at each point in the sampled density range. Typically, using the above algorithm over a mesh of points separated by an interval $\Delta\eta = 0.005$, it is possible to push the convergence rate of the calculation up to values of the order of 10^{-10}–10^{-11}.

We find that the iterative procedure outlined above does lead to a properly convergent solution of the model in a range of densities which is quite restricted with respect to the original PY domain. Actually, the number of iterations needed to achieve a given convergence rate starts to increase in a fairly sharp way beyond $\eta \simeq 0.7$. For $\eta \geqslant 0.78$ our algorithm fails to converge. More specifically, this means that it is possible to find a solution which converges uniformly with a rate, say, of 10^{-10} at all points sampled in the closed domain $0 \leqslant \eta \leqslant 0.775$. This boundary, to within an error which is at the most equal to the integration step, turns out to be almost independent of the order of the approximation. Therefore, the highest limit density consistent with the theory is predicted to lie in the range $0.775 < \eta_{\max}^{\mathrm{SCT}} < 0.780$.

Still, as a matter of principle, it cannot be excluded that such an "instability" of the algorithm is a numerical artifact due, say, to the specific choice made for the initial guess on the thermodynamic iterants. This possibility must be taken into serious account particularly at high densities,

where the input may deviate highly from the solution given by the theory. We have tried to verify this by implementing an alternative procedure which works in a *perturbative* way and does not need any external input. The integration range is now extended step by step starting from $\eta = 0$. The guess for the value of the iterants at the next added border point is in fact obtained by extrapolating the solution found before in the inner region.[7] At each stage, the algorithm can and actually does rearrange the iterants everywhere in the chosen interval as a result of the nonlocal nature of the consistency constraints. However, as one would expect, the numerical solution rapidly saturates and the influence of each new point does not back-propagate deeply inside. We verify also that the solution thus found smoothly merges into the analytical expansion of the theory about $\eta = 0$. This procedure works as long as one does not move beyond the claimed limit density $\eta_{\max}^{\mathrm{SCT}}$. In fact, upon surpassing this border, we find that the solution at lower densities, which was already well stabilized, starts to be affected in a way which no longer complies with the exact expansion of the theory in the limit of $\eta \to 0$. More specifically, the estimated iterants begin to exhibit an erratic dependence upon η with the onset of irregular ripples which gradually propagate to higher and higher densities the further the algorithm is pushed beyond $\eta_{\max}^{\mathrm{SCT}}$, until convergence is utterly lost. On this basis, we conclude that the branch detected for $\eta > \eta_{\max}^{\mathrm{SCT}}$ is not a proper solution of the self-consistent scheme.

8. RESULTS AND DISCUSSION

8.1. Equation of State

Table II reports the values of the parameters entering SCT(2), i.e., K, z, and α_2, as a function of η, which have been calculated using the above algorithm. Correspondingly, Fig. 2 shows the equation of state $Z(\eta) \equiv \beta P/\rho$ plotted as the difference

$$\Delta Z(\eta) = Z(\eta) - Z_{\mathrm{EW}}(\eta) \tag{45}$$

where $Z_{\mathrm{EW}}(\eta)$ is an analytic representation of the experimental EOS obtained through a least-square fit of a [3/2] Padé approximant to Monte Carlo and molecular dynamics data for densities in the range $0.03 \lesssim \eta \lesssim 0.46$.[26] Obviously, outside this domain, $Z_{\mathrm{EW}}(\eta)$ yields nothing but a mere extrapolation of the numerical simulation data. However, while

[7] The first guess at $\eta = 0.01$ is obtained from the analytic expansion of the theory to second order in η (see the Appendix).

Table II. SCT(2) Free Parameters as a Function of the Packing Fraction η

η	α_2	K	z
0.000	-0.155850×10^{1}	0.000000×10^{0}	0.405818×10^{1}
0.050	-0.165327×10^{1}	0.163277×10^{-2}	0.438719×10^{1}
0.100	-0.174295×10^{1}	0.831198×10^{-2}	0.476670×10^{1}
0.150	-0.181652×10^{1}	0.238151×10^{-1}	0.520607×10^{1}
0.200	-0.185194×10^{1}	0.539749×10^{-1}	0.571428×10^{1}
0.250	-0.181177×10^{1}	0.107731×10^{0}	0.630370×10^{1}
0.300	-0.164192×10^{1}	0.198716×10^{0}	0.700031×10^{1}
0.350	-0.128620×10^{1}	0.347338×10^{0}	0.787349×10^{1}
0.400	-0.714607×10^{0}	0.583069×10^{0}	0.908077×10^{1}
0.450	0.872291×10^{-1}	0.949167×10^{0}	0.108807×10^{2}
0.500	0.119971×10^{1}	0.151663×10^{1}	0.136127×10^{2}
0.550	0.285036×10^{1}	0.241251×10^{1}	0.177628×10^{2}
0.600	0.550499×10^{1}	0.387668×10^{1}	0.241766×10^{2}
0.650	0.101243×10^{2}	0.639715×10^{1}	0.344905×10^{2}
0.700	0.188859×10^{2}	0.110680×10^{2}	0.521757×10^{2}
0.750	0.373945×10^{2}	0.206764×10^{2}	0.855630×10^{2}
0.775	0.546535×10^{2}	0.294817×10^{2}	0.114255×10^{3}

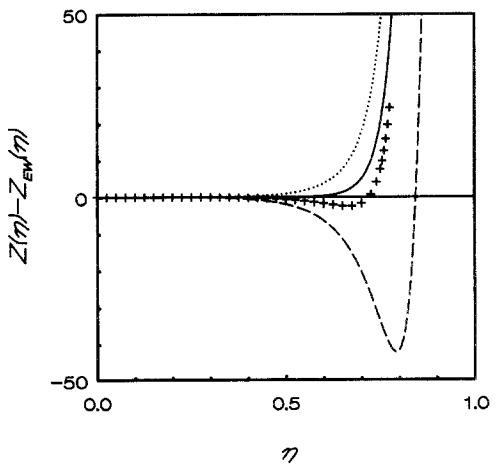

Fig. 2. Compressibility factor $Z(\eta) \equiv \beta P/\rho$ plotted as the difference to the Erpenbeck and Wood least-square fit of Monte Carlo and molecular dynamics data[26]: crosses, SCT(2); dotted line, Percus–Yevick (fluctuation route); dashed line, Percus–Yevick (virial route); continuous line, Carnahan and Starling.

there is no reason whatsoever to trust the reliability of $Z_{EW}(\eta)$ at high densities, this approximant does still provide a convenient reference for comparing different approximations with a finer resolution. In fact, in Fig. 2 we also show the PY virial and fluctuation equations of state, which, as expected, bracket the EOS predicted by the present theory at all densities. Note also that the EOS given by SCT runs very close to CS up to high densities.

Given the discussion in Section 6 of the rather different asymptotic behaviors which may be inferred for z after an analysis of the generalized set of constraints on one hand and of the bare OZ theory on the other, it is enlightening to look at the ratio $z/y(1)$ as a function of η. This quantity is shown in Fig. 3. In order to visualize the reason for the breakdown undergone by the theory at $\eta \simeq 0.78$, we first extrapolate the results given by SCT by fitting the last few points of $y(1)$ to

$$y(1) = \frac{Y}{(1-\eta)^{\alpha}} \tag{46}$$

This two-parameter form with $Y \simeq 0.69$ and $\alpha \simeq 2.84$ reproduces the high-density branch of $y(1)$ with fair accuracy. The derivative of Eq. (46) yields through Eq. (14) the inverse compressibility. Obviously, for $\eta > 0.78$ this fit will not produce an entirely consistent solution for the thermodynamics of the system. In fact, upon calculating z via the OZ route given in Eq. (11) we obtain a branch which, consistently with Eq. (44), extrapolates to zero (see Fig. 3). Alternatively, upon using Eq. (41), it becomes rather manifest

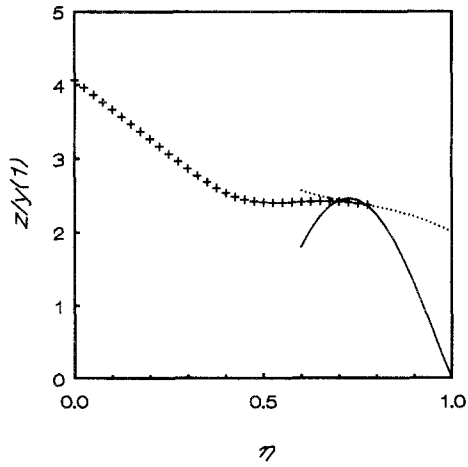

Fig. 3. The ratio $z/y(1)$ as a function of the packing fraction η and asymptotic extrapolation of SCT(2) data (crosses) performed by using Eq. (46) together with Eq. (11) (continuous line) and Eq. (41) (dotted line), respectively.

that the theory is facing a rather sharp bifurcation since the branch obtained by solving this last equation behaves differently as $\eta \to 1$, smoothly approaching 2 in agreement with Eq. (43). Note that for $\eta \gtrsim 0.7$, SCT appears to have already entered the asymptotic regime where, initially, the two routes do in fact lead to consistent estimates. Therefore, the failure of the numerical algorithm at $\eta \simeq 0.77$–0.78 is precisely in relation to the irremediable relative divergence of the two branches. We shall discuss in the following section the possible physical foundations of such a finding.

8.2. On the Breakdown of the Theory for $\eta \gtrsim 0.78$

The location of the higher boundary predicted by the theory for the existence of a solution satisfying the threefold condition of thermodynamic consistency does not fall far from the closest-packing point ($\eta_{CP} \simeq 0.74$), corresponding to the state of maximal density which is available through an ordered arrangement of spheres. We surmise that this is not merely accidental. In fact, an even closer "coincidence" appears to support this feeling: the estimated border for the existence of a solution within SCT(2) lies just above the *least* upper bound for the densest packing of spheres obtained so far, viz., $\eta_R = 0.7796...$,[8] a result found by Rogers[27] in 1958. We recall that η_R is indeed the density corresponding to a *local* tetrahedral arrangement where four spheres touch one another at a time and thus cannot move closer together. However, it is also well known that this optimal configuration cannot be reproduced indefinitely on a global scale since regular tetrahedra do not fill three-dimensional space.[9] Hence, upon adding for instance new spheres to an initial seed of four ones, larger voids than those provided by an ideal tetrahedral network must open up at some stage here and there, ultimately leading to a structure whose density is actually lower than η_R. On a microscopic level, such voids may also be viewed as the average configurational outcome of a class of many-body collisional events tending to keep spheres apart, one from another. These effects, even after the statistical averaging, should also emerge in the direct correlation function which, as a matter of principle, contains all the relevant information about the local order building up in the system on a pair level. And, indeed, their presence may be traced back to some features which are found in the behavior of the DCF even at low densities.[24] In fact, at variance with $d_2(x)$, the next term in the density expansion of the tail function, $d_3(x)$, also attains negative values in the range $1.25 \lesssim x \leqslant 2$, before

[8] The exact result is $\eta_R = \sqrt{2} \cdot [3 \arccos(1/3) - \pi]$.

[9] In fact, the dihedral angle of a regular tetrahedron is not a submultiple of 2π.

vanishing exactly for distances greater than two hard-sphere diameters. Within a framework analogous to the one previously discussed in Section 2, such a negative tail may be interpreted as the result of a net average repulsion acting between a couple of spheres well outside the range σ covered by the mechanical hard-sphere interaction (see footnote 3). As already stressed before when discussing the positive component in the DCF, this "thermal repulsion" is again the outcome of a collective interplay involving all of the remaining particles, which, to some extent, act in such a way as to loosen the rigidity of the cage stabilized at shorter distances by the effects giving rise to the stronger positive tail. It is clear that the importance of such features in the DCF should increase with the density. The existence of a negative tail has been in fact postulated in density-functional theories of the freezing[28] and of the liquid-glass transition[29] for hard spheres. But an even more stringent argument invoking its presence in the DCF has been recently formulated by Song *et al.*[3] These authors note that, on approaching the thermodynamic singularity associated with the state of maximum packing, the pressure of the system should clearly diverge. On the other hand, density fluctuations (and, correspondingly, the isothermal compressibility) should eventually vanish. As a result, the direct correlation function must become infinitely long ranged, vanishing asymptotically from the negative side!

Retrospectively, the very absence of this last feature in a model single-Yukawa DCF naturally accounts (while not being perhaps the only cause) for the overshooting of the highest density attainable by the system within SCT. In fact, upon neglecting any extra contribution outside the core apart from an *attractive* positive tail, the present scheme unbalances the relative weight associated with the two types of short-range correlation effects discussed above. As a result, at a given pressure P the theory produces a macroscopic state characterized by a *tighter* packing than that which actually occurs, say, in a numerical simulation experiment. Furthermore, the absence of a negative tail in our ansatz for the DCF precludes the theory from driving the thermodynamic properties to a proper singularity for $\eta = \eta_{\max}^{\mathrm{SCT}}$. Notwithstanding these deficiencies, the present scheme predicts the existence of a higher boundary well beneath $\eta = 1$ on account of the failure to achieve complete thermodynamic consistency. Altogether, this result appears as a nontrivial, soundly physical improvement over the typically "one-dimensional" features ($\eta_{\max}^{\mathrm{PY}} = 1$) which are regrettably conveyed into a three-dimensional formulation by the PY theory.

8.3. The Radial Distribution Function and the Point of Random Close Packing

As recalled in the Introduction, the first minimum in the PY radial distribution function touches zero for a value of the packing fraction $\eta_{\min}^{PY} \simeq 0.612$. From there on, with increasing density, the minimum turns into an increasingly negative dip. Since, by definition, the RDF should be positive for all x, the solution of the PY approximation is not considered physically acceptable for $\eta > \eta_{\min}^{PY}$, "despite the fact that the equation of state shows no discontinuity whatever at this density, and continues smoothly up to $\eta = 1$."[30] Still, the vanishing of the first minimum in the RDF is not without relevance as far as the type of local order established in the system is concerned. In fact, at the above density the first coordination shell eventually acquires a well-defined identity and stability relative to the outer shells of neighbors. Correspondingly, it becomes possible to state unanbiguously how many particles give rise to the *cage* confining a central tagged particle anywhere in the system. Within SCT(2), where the value of the calculated density is $\eta_{\min}^{SCT(2)} \simeq 0.635 \pm 0.005$, the coordination number calculated from the RDF (which is shown in Fig. 4) turns out to be 12.0,[10] as one would expect. Twelve is in fact the "kissing number," i.e., the maximum number of spheres which can be arranged around a central one in such a way that each of the surrounding particles may actually touch the central one.

[10] The PY value at $\eta = \eta_{\min}^{PY}$ is 12.3.

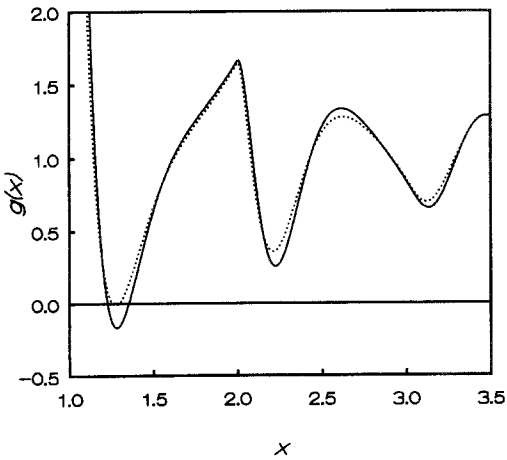

Fig. 4. Radial distribution function $g(x)$ for $\eta = 0.635$: dotted line, SCT(2); continuous line, Percus–Yevick.

In a different but still related sense, we also note that the first shell happens to saturate at a density which, within both numerical and experimental accuracy, essentially drops over the currently estimated value of the RCP threshold $\eta_{RCP} = 0.64 \pm 0.02$.[10] This happenstance is undoubtedly quite suggestive: the onset of the topological condition described above is, apparently, revealed as the *equilibrium* facet of the *nonequilibrium* aggregation phenomenon, leading, in either a "real-life" or numerical experiment, to the state of random close packing. Such a hypothesis is in fact justified by a number of correlated structural and dynamical facts. In the density region in which we are concerned, configuration relaxation times become extremely long: particles get locally trapped and, consistently, their diffusion coefficient sharply drops to zero.[31,32] Therefore, establishing complete equilibrium in a concrete physical sample may well turn into an increasingly difficult task. On this basis, upon compressing or compacting a system of hard spheres within a container, it is not unlikely to see the gradual merging of the equilibrium branch into a nonequilibrium branch terminating at the point of RCP. Following this idea, it is interesting to compare the structure of the fluid at RCP (or in a state close to RCP) with the type of order emerging in the RDF given by the present equilibrium theory at similar densities. A dense random packing of spheres can be simulated on a computer by a sequential addition technique somewhat analogous to the experimental method of vapor deposition at absolute zero.[33] In Fig. 5 we show the RDF calculated through such a technique from the coordinates of 3999 particles following a "global"

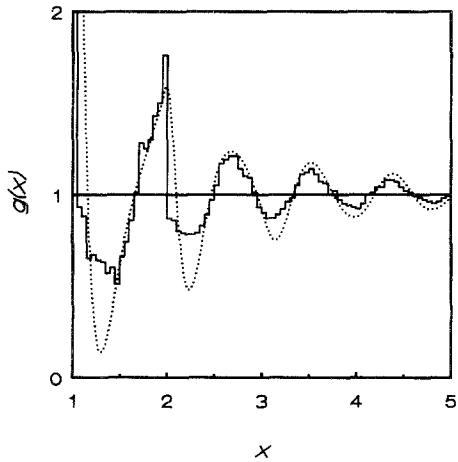

Fig. 5. Comparison between SCT(2) radial distribution function $g(x)$ for $\eta = 0.61$ (dotted line) and Bennett's RDF (histogram) obtained on a computer by a static sequential addition technique.[33]

building criterion: any new particle is added at that surface site—formed by three preexisting kissing spheres—which is closest to the center of the original seed cluster (typically, an equilateral triangle of three particles in contact). The dotted curve is the RDF evaluated within SCT(2) at $\eta = 0.61$ corresponding to the value of the cluster packing fraction extrapolated to infinite volume so as to eliminate size and boundary effects. Taking into account the profound difference between the methods used for obtaining the above quantities, the overall mutual agreement seems unexpectedly good. The shape of the maxima in the cluster RDF is reproduced by the theory with fairly quantitative accuracy. In particular, the shoulder emerging on the inside of the second peak is notoriously associated with the frequent occurrence of typical tetrahedral arrangements where two tetrahedra share a common base (a trigonal bipyramid configuration) or just a common side. In the former case, the two tetrahedron apices are separated by a distance $2\sqrt{6}/3 \simeq 1.633$, while in the latter situation the two coplanar equilateral bases have opposite apices separated by a distance $\sqrt{3} \simeq 1.732$. At variance with the peaks, valleys as predicted by the theory are systematically deeper. Actually, such a discrepancy can be traced back to the nature of the addition algorithm, which, on the average, generates geometries where each particle rests on three "older" spheres and in turn supports three "younger" particles. This type of local arrangement leads in general to six "close" contacts, and to a lower number of "near" contacts (such that particles nearly touch) which are distributed over slightly greater distances.[34] On the other hand, the theory, in virtue of the thermal equilibrium sampling effectively implied over the whole spectrum of allowed configurations, models a more uniform local distribution of particle separations and does not obviously distinguish between close and near contacts. Apart from this marginal aspect, the close similarity of the two structure functions gives support to our conjecture about the nature of the random close-packing state and its corresponding signature in the equilibrium properties of the system.

As already stated, for densities $\eta > \eta_{\min}^{\mathrm{SCT}(2)}$ the information contained in the RDF is no longer reliable. The modification of the PY ansatz for the DCF outside the core with a simple Yukawa tail is not adequate for removing entirely the presence of regions where the RDF becomes negative. What one would indeed expect to happen in the RDF from $\eta_{\min}^{\mathrm{SCT}(2)}$ on is an increasing flattening of the function down to zero in a range expanding progressively on both sides of the point where the RDF initially touched zero. Indeed, in one dimension, where the PY closure is exact, the RDF is described for $1 < x < 2$ by just one single exponential, which, at high densities, sharply flattens to zero well before the rise of the second shell at $x = 2$.

9. CONCLUDING REMARKS

In this paper we have analyzed the predictions given by a self-contained OZ approach to the structure and thermodynamics of hard spheres with particular emphasis on the properties of the system at high density. The scheme is based upon an approximation for the tail function $d(x)$, which, outside the core, reduces to a one-Yukawa form *à la* Waisman. The parameters entering our ansatz for $d(x)$ are calculated by resorting to a generalized closure, which rests upon the requirement of full consistency between thermodynamics and structure at a pair level and on the continuity properties of the tail function at contact. The theory has been solved numerically by an iterative procedure, but, at variance with other well-known approximations, a solution has been found only over a restricted density range, i.e., for values of the packing fraction not greater than 0.78. The prediction of a higher boundary, where the physical branch discontinuously terminates, is in fair suggestive agreement with the existence of a state of maximum packing for a system of hard spheres. However, on account of the incompleteness of the ansatz for the tail function outside the core, the breakdown of the theory is not sustained by a singularity in the thermodynamic properties and the radial distribution function still shows unphysical negative regions. Therefore, we believe that a more definite statement about the envisaged relation between the boundary predicted by SCT and the closest-packing point of hard spheres may only come after some further analysis to be carried out on a more flexible scheme such as that potentially provided by a two-Yukawa approximation for $d(x)$ outside the core.[11] A deeper elucidation of this point, which is also relevant to the question concerning the description of the system in the region where a fluid-to-solid phase transition is observed in numerical simulation experiments, is left to a forthcoming paper.

APPENDIX. LOW-DENSITY EXPANSION

As already discussed in ref. 2, upon expanding to order η^2, Eq. (11), we find

$$z^{(0)} \equiv \lim_{\eta \to 0} z(\eta)$$
$$= \{3K_2 + [3K_2(6 - 5K_2)]^{1/2}\}(3 - 4K_2)^{-1} \qquad \text{(A.1)}$$

[11] The need to resort to a better approximation for the DCF outside the core such as that provided by a two-Yukawa form has been stressed also by Zhou and Stell, who in ref. 22 note that "the one-Yukawa fit for $c(r)$, $r > \sigma$, is not accurate enough to support self-consistently an extremely accurate equation of state."

where K_2 is defined through Eq. (26a). Equation (A.1) already ensures the consistency between the virial and fluctuation routes to the evaluation of the EOS to second order in the density. The residual conditions arising from the two zero-separation theorems lead to one more relation between $z^{(0)}$ and K_2, whose form, however, depends on the approximation adopted for the tail function inside the core and, more specifically, on the value set for the upper summation index N in Eq. (7). Upon expanding Eqs. (21) and (22) and after making convenient use of Eqs. (33)–(35), we find

$$\mathrm{SCT}(2) \Rightarrow z^{(0)} = -\tfrac{50}{17} - 2\ln(K_2/17) \tag{A.2}$$

$$\mathrm{SCT}(3) \Rightarrow z^{(0)} = -\tfrac{151}{68} - \tfrac{3}{2}\ln(K_2/17) \tag{A.3}$$

$$\mathrm{SCT}(4) \Rightarrow z^{(0)} = -\tfrac{320}{153} - \tfrac{4}{3}\ln(K_2/17) \tag{A.4}$$

Each of these equations, when coupled with Eq. (A.1), leads to a transcendental equation for K_2 which can be solved numerically. The fourth virial coefficient is related to K_2 via the equation

$$B_4/(\tfrac{1}{4}B_2)^3 = 16 + 4K_2 \tag{A.5}$$

The results we thus find in each scheme are summarized in Table I. Note that the first entry for $z^{(0)}$ (6.450) is obtained from Eq. (A.1) when K_2 is calculated through Eq. (A.5) using the exact value for the fourth virial coefficient. We include this number as a reference value for the estimates following from SCT. We also note that this result for $z^{(0)}$ is pretty close to but still higher than the value (5.998) derived through an external fitting procedure which, after fixing $c(1^+)$ to the value known exactly at order ρ^2, evaluates $z^{(0)}$ by requiring the L_2 norm of the difference between the Yukawa tail and $d_2(x)$ outside the core to be as small as possible.[35] We note that a faster spatial decay of the DCF is more consistent with the behavior of $d_2(x)$ which is known to vanish for distances greater than $\sqrt{3}$.

ACKNOWLEDGMENTS

This work was supported by the Ministero dell' Universita' e della Ricerca Scientifica e Tecnologica, and by the Consorzio Interuniversitario Nazionale per la Fisica della Materia.

REFERENCES

1. G. Giunta, C. Caccamo, and P. V. Giaquinta, *Phys. Rev. A* **31**:2477 (1985).
2. P. V. Giaquinta, G. Giunta, and G. Malescio, *Phys. Rev. A* **35**:3564 (1987).
3. Y. Song, R. M. Stratt, and E. A. Mason, *J. Chem. Phys.* **88**:1126 (1988).

4. M. Alexanian, *Phys. Rev. A* **37**:4527 (1988).
5. M. de Llano, *Phys. Rev. A* **37**:4529 (1988).
6. W. G. Hoover and F. H. Ree, *J. Chem. Phys.* **49**:3609 (1968), and references contained therein.
7. J. K. Percus and G. J. Yevick, *Phys. Rev.* **110**:1 (1957).
8. M. S. Wertheim, *Phys. Rev. Lett.* **10**:321 (1963).
9. E. Thiele, *J. Chem. Phys.* **39**:474 (1963).
10. J. G. Berryman, *Phys. Rev. A* **27**:1053 (1983).
11. J. P. Hansen and I. R. McDonald, *Theory of Simple Liquids*, 2nd ed. (Academic Press, London, 1986).
12. R. D. Groot, J. P. van der Eerden, and N. M. Faber, *J. Chem. Phys.* **87**:2263 (1987).
13. J. K. Percus, in *The Liquid State of Matter: Fluids, Simple and Complex*, E. W. Montroll and J. L. Lebowitz, eds. (North-Holland, Amsterdam, 1982).
14. E. Waisman, *Mol. Phys.* **25**:45 (1973).
15. N. F. Carnahan and K. E. Starling, *J. Chem. Phys.* **51**:635 (1969).
16. W. G. Hoover and J. C. Poirier, *J. Chem. Phys.* **37**:1041 (1962).
17. E. Meeron and A. J. F. Siegert, *J. Chem. Phys.* **48**:3139 (1968).
18. J. K. Percus, in *The Equilibrium Theory of Classical Fluids*, H. L. Frisch and J. L. Lebowitz, eds. (Benjamin, New York, 1964), Chapter II, p. 33.
19. M. W. Liao and J. K. Percus, *Mol. Phys.* **56**:1307 (1985).
20. D. Henderson and E. W. Grundke, *J. Chem. Phys.* **63**:601 (1975).
21. J. S. Høye and G. Stell, *Mol. Phys.* **32**:195 (1976).
22. Y. Zhou and G. Stell, *J. Stat. Phys.* **52**:1389 (1988).
23. G. Stell, *Physica* **24**:517 (1963).
24. F. H. Ree, R. N. Keeler, and S. L. McCarthy, *J. Chem. Phys.* **44**:3407 (1966).
25. B. R. A. Nijober and L. van Hove, *Phys. Rev.* **85**:777 (1952).
26. J. J. Erpenbeck and W. W. Wood, *J. Stat. Phys.* **35**:321 (1984).
27. C. A. Rogers, *Packing and Covering* (Cambridge University Press, Cambridge, 1964).
28. P. Tarazona, *Phys. Rev. A* **31**:2672 (1985).
29. Y. Singh, J. P. Stoessel, and P. G. Wolynes, *Phys. Rev. Lett.* **54**:1059 (1985).
30. M. Wertheim, in *The Equilibrium Theory of Classical Fluids*, H. L. Frisch and J. L. Lebowitz, eds. (Benjamin, New York, 1964), Chapter II, p. 281.
31. L. V. Woodcock, *Ann. N. Y. Acad. Sci.* **371**:274 (1981).
32. R. J. Speedy, *Mol. Phys.* **62**:510 (1987).
33. C. H. Bennett, *J. Appl. Phys.* **43**:2727 (1972).
34. J. D. Bernal and J. Mason, *Nature* **188**:910 (1960).
35. S. Ciccariello, *Phys. Lett. A* **114**:313 (1986).